Polyamide 6 Composites Reinforced with Silicon Nitride Whiskers: Synthesis, Interface Interaction, and Mechanical Properties

Lanjie Li,[1,2] Guisheng Yang[1,3]

[1]*CAS Key Laboratory of Engineering Plastics, Joint Laboratory of Polymer Science and Materials, Institute of Chemistry, The Chinese Academy of Sciences, Beijing 100080, People's Republic of China*
[2]*Graduate School, the Chinese Academy of Sciences, Beijing 100039, People's Republic of China*
[3]*Shanghai Genius Advanced Materials Co., Ltd., Shanghai 201109, People's Republic of China*

Received 8 March 2009; accepted 20 April 2009
DOI 10.1002/app.30708
Published online 4 November 2009 in Wiley InterScience (www.interscience.wiley.com).

ABSTRACT: In this study, polyamide 6 (PA6)/silicon nitride whisker (SNW) composites were fabricated via *in situ* hydrolytic ring-opening polymerization of ε-caprolactam. By this novel method, SNWs can be dispersed uniformly in PA6 matrix. The interface interaction between SNW and PA6 was investigated, and the reinforcing efficiency of SNW on PA6 was evaluated. It was revealed by Fourier transform infrared spectroscopy that a large amount of polar groups, such as —SiOH, —NH, and —NH_2, were present on the SNWs, by which hydrogen bonding and covalent bonding can be formed at interface. Mechanical test showed that at a loading of 5.0 wt % SNW, the tensile strength, tensile modulus, flexural strength, flexural modulus, and impact strength of PA6/SNW composite were 37.9, 80.5, 60.3, 73.9, and 64% higher than those of neat PA6, respectively. © 2009 Wiley Periodicals, Inc. J Appl Polym Sci 115: 3376–3384, 2010

Key words: silicon nitride whiskers; polyamide 6; interface interaction; composites; mechanical properties

INTRODUCTION

Whiskers are a kind of single crystal with high degree of structural perfection, elongated shape, and very thin diameter.[1] Because of the limited internal flaws, whiskers are generally known to exhibit high modulus and strength close to the maximum theoretical value expected from the theory of elasticity.[2] For this reason, inorganic whisker-reinforced polymer composites have emerged as a new class of high-performance composites in recent years. Whiskers, such as aluminum borate ($Al_8B_4O_{33}$),[3–7] zinc oxide (ZnO),[8–10] silicon nitride (Si_3N_4),[11–13] silicon carbide (SiC),[12,14] calcium carbonate ($CaCO_3$),[15] potassium titanate ($K_2Ti_6O_{13}$),[2,16–22] aluminum oxide (Al_2O_3),[23] and aluminum nitride (AlN),[24,25] have been used as reinforcement filler in various polymer system. Dramatically improved strength, modulus, and wear resistance of polymer/whisker composites have been reported by many researchers.

Polyamide 6 (PA6) is used in a wide range of engineering applications because of its attractive combination of good mechanical properties and processability.[21] To further widen its application as metal substitute, higher strength and modulus are often required. Therefore, various fiber reinforcements, such as glass fiber and carbon fiber, are frequently added to polyamides.[26–31] One disadvantage of using commercial fibers is the enhancement of the viscosity. Moreover, the fiber content has to be more than 30% to get acceptable reinforcing effect. This leads to difficulties during processing of the composites.[1] In addition, the fiber-reinforced composites are usually anisotropic in mechanical properties and heterogeneous, depending on the fiber size and orientation, which make them only suitable for structural application.

It is therefore of interest to find alternatives for the conventional short fibers. According to the theories of short fiber composites, the composites reinforced with thinner, stronger fibers can be anticipated to achieve much higher mechanical properties.[18] It's known that the strength of whiskers is 10 times higher than that of fibers, whereas the size of the whiskers is orders of magnitude smaller.[1] Therefore, whiskers are reckoned as more effective reinforcements than traditional fibers. Different from fiber-reinforced composites, the whisker composites have relatively isotropic and homogeneous properties and are more suitable for preparing small but precisely dimensioned parts, which are generally difficult to be reinforced by using fibers. In recent years, different whiskers have been used to reinforce polyamides. Shi et al.[8] used zinc oxide whisker to

Correspondence to: G. Yang (ygs@geniuscn.com).

reinforce PA6 and studied the fracture behavior of the composites. Besides, potassium titanate whiskers[21,22] and aluminum borate whiskers[7] have also been used as reinforcements in polyamide composites. In this study, silicon nitride, a kind of ceramic whisker, is used to reinforce PA6.

Among numerous inorganic whiskers, silicon nitride whisker (SNW) is the one that possesses the highest strength and hardness because of the strong covalent bonding between each atom.[32] Huttinger and Pierchnick[33] reported that the tensile strength and Young's modulus of α-Si3N4 whiskers of a few micrometers in diameter were 30–50 GPa and 550–750 GPa, respectively. Iwanaga and Kawai[32] also reported that the tensile strength of α-Si3N4 whisker of 300 nm in diameter was as high as 59 GPa. The mechanical strength of SNW can be comparable to that of carbon nanotube. Therefore, SNW can show much better reinforcing efficiency than other whiskers. In the past, SNW had been used to reinforce dental resin by Eichmiller and coworkers,[11–13] and its ability in increasing modulus, strength, and wear resistance of composites had been confirmed.

Uniform dispersion of whiskers in matrix is very important for satisfactory reinforcement. However, because of their ultrathin diameter and high aspect ratio, whiskers prefer to agglomerate and entangle, which makes it extremely difficult to achieve uniform dispersion of whiskers. Traditional twin-screw extrusion process cannot realize uniform dispersion of ultrathin fillers, not to mention whiskers with high aspect ratio. In addition, this method may lead to an adverse effect: the crystalline structure of whiskers may be destroyed during processing. To avoid this side effect and improve the dispersion of whiskers in matrix, *in situ* polymerization is often used.[34]

In this study, a novel preparation technique, *in situ* hydrolytic ring-opening polymerization (IS-HROP) of ε-caprolactam, is adopted to fabricate PA6/SNW composites. By this technique, the agglomeration and entanglement of whiskers can be effectively solved. Besides, emphasis has also been focused on the strong interface interaction between PA6 and SNW, which helps explain the excellent reinforcing efficiency of SNW on PA6.

EXPERIMENTAL

Materials

SNW was obtained from Hefei Kaier Nanometer Technology and Development, China. Commercial grade ε-caprolactam was bought from Nanjing Oriental Chemical Company, China. Analytical grade adipic acid, *n*-aminocapric acid, and formic acid were bought from National Reagent Group, China.

Preparation of PA6/SNW composites

A desired amount of SNW was dispersed into a solution of water and ε-caprolactam and then mixed under strong ultrasonic oscillation for half an hour. To control the molecular weight of PA6, a predetermined amount of adipic acid was added to the mixture. The mixture was transferred to a 2-L steel reactor equipped with nitrogen inlet and mechanical mixer. The air in the reactor was purged completely using nitrogen. The system was heated to 250–260°C and the pressure was increased to 2.0–3.0 MPa simultaneously. Prepolymerization was performed under this condition for 6 h. Then, the pressure was decreased to normal atmosphere by discharging water vapor slowly, and the reaction was further carried out at atmospheric pressure for 2 h. Finally, postpolymerization was carried out at 260–280°C and 600–1000 Pa for half an hour. PA6/SNW composites were then obtained and were denoted as PA6SNW-*X* (*X* means the weight percentage of SNW in the composites). For the purpose of comparison, neat PA6 was also prepared without adding SNW.

To show the advantage of IS-HROP in fabricating PA6/whisker composites, a control composite was also prepared via traditional *in situ* polymerization as described by Ou et al.,[34] that is, *in situ* polymerization of ε-caprolactam with *n*-aminocapric acid as initiator. The SNW content in the control composite was 5.0 wt %.

The sample codes, formulation, and the actual SNW content in final composites are given in Table I.

Before test, all samples were dried under vacuum at 100°C for 48 h. Thermogravimetric analysis showed that there was no obvious difference between the theoretical and the actual SNW content of the samples. The treatment processes of all samples were identical to ensure comparability of the test results.

Separation of PA6-grafted SNW

PA6SNW-5 (1 g) was dissolved in 10 mL of formic acid, and then the whiskers were separated by centrifugation. The same dissolution-centrifugation process was repeated eight times to make sure that the free PA6 was removed completely. Then, the whiskers obtained were dried in a vacuum oven at 100°C for 24 h to remove the residual formic acid.

Characterization

A Waters-991 gel permeation chromatography instrument was used to evaluate the weight-average molecular weight ($\overline{M}_w$) and the polydispersion ($\overline{M}_w/\overline{M}_n$) of PA6, where $\overline{M}_n$ is the number-average molecular weight, by calibration with a PA6 standard. The measurements were performed at 35°C on

TABLE I
Formulation, Sample Codes, and Composition of the Prepared Samples

Sample code	ε-Caprolactam (g)	SNW (g)	Water (g)	Adipic acid (g)	*n*-Aminocapric acid (g)	SNW (wt %)	
						Theoretical[a]	Experimental[b]
PA6	2000	0	200	20.0	0	0	0
PA6SNW1	1980	20	400	19.8	0	1.0	1.03
PA6SNW3	1940	60	400	19.4	0	3.0	3.07
PA6SNW5	1900	100	600	19.0	0	5.0	5.12
Control composite	1800	100	0	19.0	100	5.0	5.08

[a] The weight percent of SNW was calculated assuming full conversion of ε-caprolactam.
[b] The experimental value was calculated by measuring the residue after the samples were sintered in a muffle furnace at 800°C for an hour.

polymeric solutions in *m*-cresol ($c = 0.5$ g/dL). All samples were solved by *m*-cresol and were filtered through a filter to remove SNW and SNW-bound PA6. PA6 in the filtrate was precipitated by acetone and dried under vacuum at 80°C for 12 h.

The micromorphology of as-received SNW and its dispersion in composites were observed using field emission scanning electron microscopy (FE-SEM; Sirion 200) at an acceleration voltage of 5 kV. All samples for FE-SEM were gold-sputtered for 50 s.

X-ray diffraction (XRD) analysis was performed on a Rigaku D/Max-III X-ray diffraction analyzer equipped with a rotating-anode generator system using Cu Kα ($\lambda = 0.15406$ nm) radiation at an operating current of 200 mA with 2θ varying between 5° and 80°. The scanning speed was 1°/min and the step size was 0.05°.

Fourier transform infrared spectroscopy (FTIR; Nicolet 170SX) was used to determine the chemical composition of SNW and PA6-grafted SNW (SNW-*g*-PA6) in the range of 400–4000 cm^{-1} with a resolution of 4 cm^{-1}. A minimum of 32 scans were signal-averaged.

For mechanical tests, the samples were directly injection-molded into standard test specimens according to ASTM procedures. Tensile tests were performed using an Instron Universal Testing machine series 1122 according to ASTM D 638 at a crosshead speed of 50 mm/min. Bending tests were carried out using the same instrument according to ASTM D 790 at a crosshead speed of 5 mm/min. The Izod impact strength was measured according to ASTM D 256 using an Izod machine Model CSI-137D.

RESULTS AND DISCUSSION

Strength and modulus of SNW

For designing whisker-reinforced composites, it is important to evaluate the strength of whiskers because there is a size effect influencing the strength of whiskers. It is well known that the strength of single-crystal whiskers increases with decreasing whisker diameter, because the smaller the diameter of the whiskers, the fewer the crystal defects in the whiskers.[32]

Figure 1 shows the SEM pictures of as-received SNW at different magnifications. Figure 1(A) shows that the SNWs have regular rod-like shape and are 10–30 μm in length. It can be seen from Figure 1(B) that the SNWs are 150–250 nm in diameter and the average diameter is about 200 nm. The average aspect ratio is evaluated to be about 80–100.

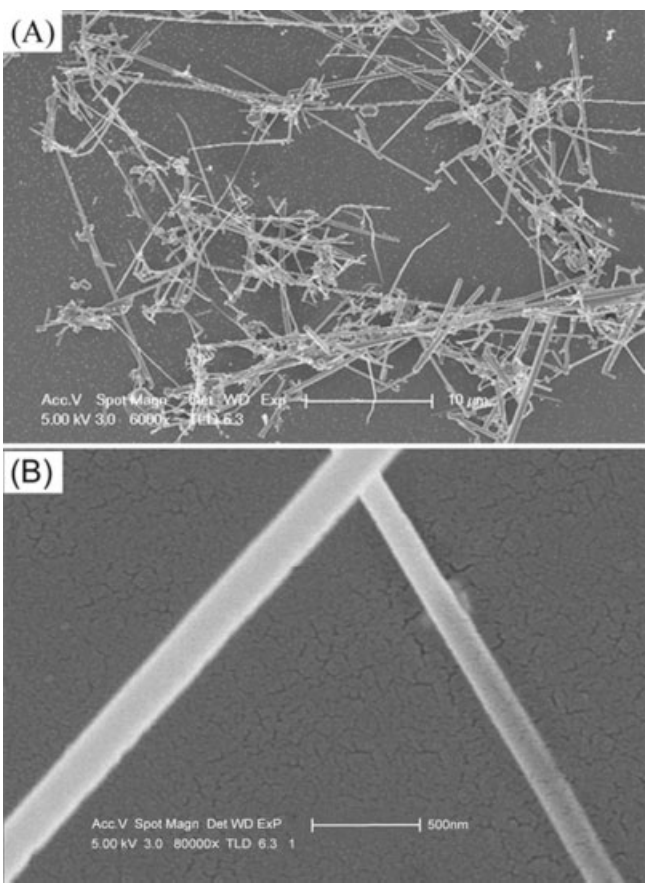

Figure 1 SEM images of as-received SNWs at different magnification. The sample for SEM was prepared by dispersing SNWs in ethanol and then dropping on a glass plate.

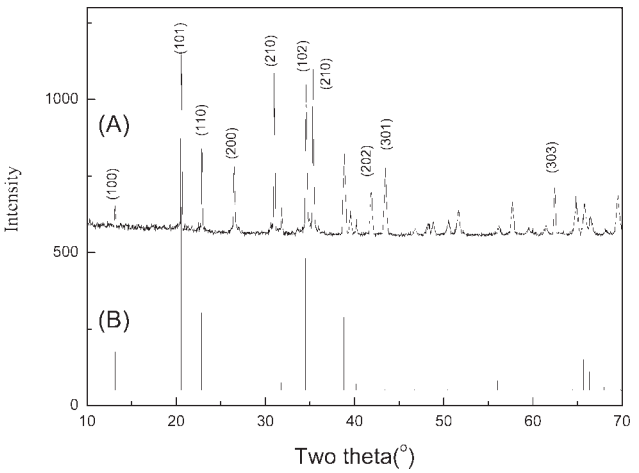

Figure 2 (A) XRD patterns of as-received SNW and (B) stick pattern of α-Si_3N_4 crystals obtained from single-crystal calculation and the Inorganic Crystal Structure Database (ICSD).

One of the most important reasons for the high strength of whiskers is their perfect crystal structure. Figure 2 shows the XRD patterns of SNW and the stick pattern of α-Si_3N_4 single crystals obtained from single-crystal calculation and the Inorganic Crystal Structure Database (ICSD). It is obvious that the SNW used in this study is α-form Si_3N_4. The diffractogram in Figure 2(A) shows very sharp peaks, confirming the perfect crystal structure of SNW.

For single-crystal whiskers, it is extremely difficult to measure their strength and modulus because of their ultrathin size. The relationship between the strength and diameter of α-Si_3N_4 whisker has been established by Iwanaga and Kawai's[32] work. Through a sensitive procedure, Kawai has measured the strength of α-Si_3N_4 whisker with different diameters. It has been reported that the strength of α-Si_3N_4 whisker with a diameter of 300 nm is about 59 GPa. Huttinger et al.[33] reported that the Young's modulus of α-Si_3N_4 whisker of a few micrometers in diameter is 550–750 GPa. Because the α-Si_3N_4 whiskers used in this study have smaller diameter, higher strength and modulus can reasonably be expected.

Dispersion of SNWs in PA6 matrix

The dispersion of whiskers in polymer matrix is very important for a satisfactory reinforcing efficiency, because only when the whiskers are dispersed uniformly in polymer matrix, each of them can bear stress evenly when load is added. However, because of the high aspect ratio and ultrafine structure, whiskers prefer to agglomerate or entangle. Figure 3 shows the SEM picture of SNW powder. It is obvious that SNWs mainly exist in the form of large agglomerates. Therefore, it is very difficult to realize uniform dispersion of these whiskers in PA6 matrix.

It has been proven that traditional melt-mixing method by twin-screw extruder cannot realize uniform dispersion of nanofillers, not to mention the whiskers with high aspect ratio.[34] To realize uniform dispersion of whiskers, *in situ* polymerization was adopted to prepare PA6SNW composites in this work.

In situ polymerization is a method in which fillers or reinforcements are dispersed in monomer first and then this mixture was polymerized using the technique similar to bulk polymerization.[34] For PA6, there are two typical kinds of *in situ* polymerization: (i) *in situ* hydrolytic ring-opening polymerization of ε-caprolactam under high pressure and high temperature in the presence of water and (ii) polycondensation of ε-caprolactam with aminocaproic acid as initiator. In this study, PA6/SNW composites have been prepared via these two methods, and the dispersion state of SNW in the composites fabricated by these two processes was evaluated.

SEM pictures of PA6SNW-5 prepared via IS-HROP are presented in Figure 4. From low magnification [Fig. 4(A)] to high magnification [Fig. 4(B)], no agglomeration of SNW can be found, indicating the uniform dispersion of SNW in PA6 matrix.

As comparison, the SEM images of the control composite prepared via polycondensation of ε-caprolactam under normal atmosphere are shown in Figure 5. It can be easily found that obvious agglomeration of SNWs exists, indicating that the dispersion of whiskers in the control composites is very poor.

By the comparison between Figures 4 and 5, it can be concluded that IS-HROP is an effective method to fabricate PA6/whisker composite with uniform dispersion. The success of this method mainly lies in the fact that the polymerization was performed in the presence of high-temperature boiling water, which can effectively prevent SNWs from precipitating and agglomerating, and also help disentangle the coil of whiskers.

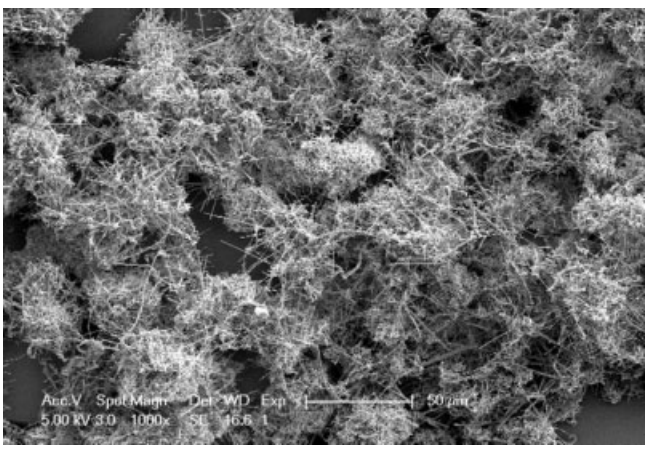

Figure 3 SEM image of SNW at low magnification, showing the agglomeration and entanglement between whiskers. SNW powder was directly used for SEM observation.

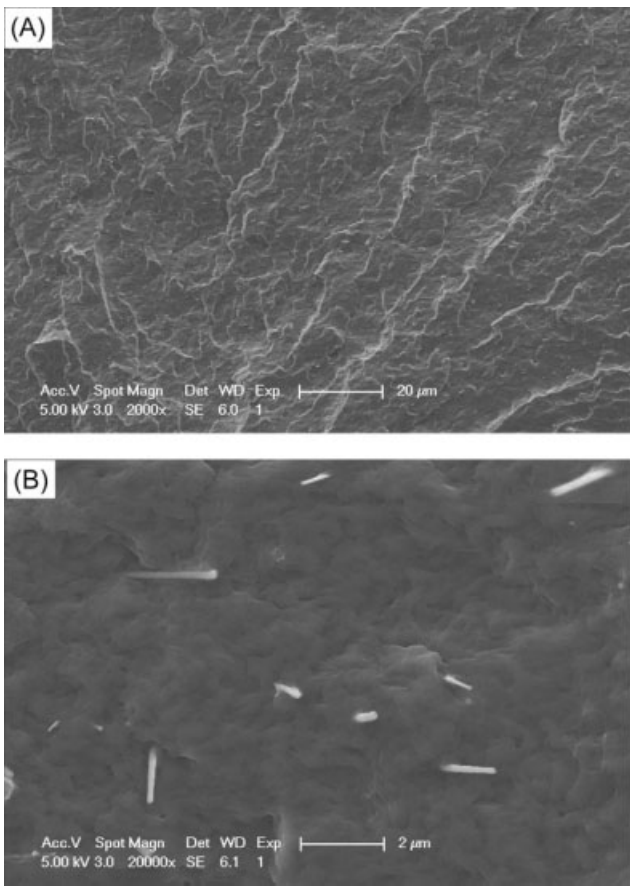

Figure 4 SEM picture of PA6/SNW composite, showing the uniform dispersion of SNW in PA6 matrix. The loading of SNW in the composite is 5.0 wt %.

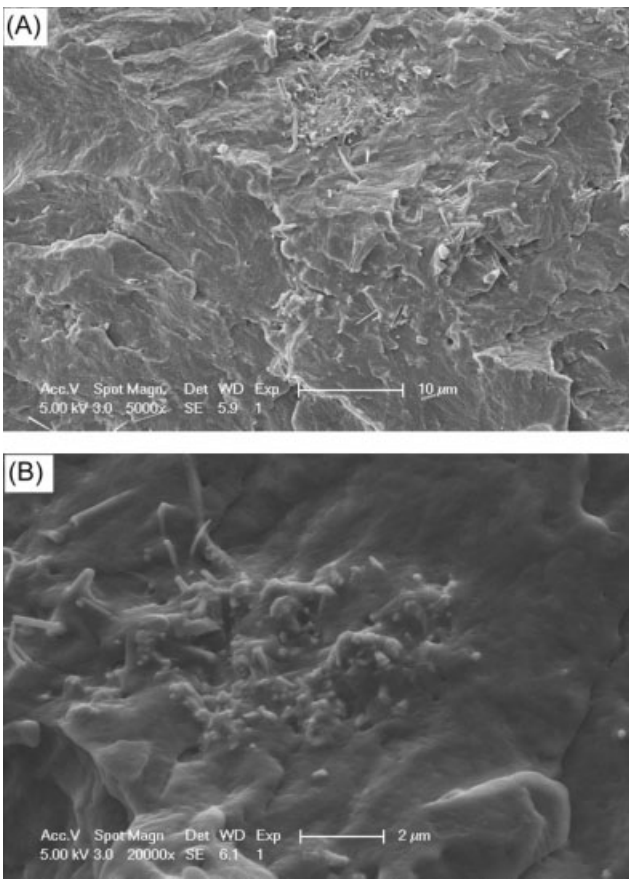

Figure 5 SEM images of the control composite prepared via polycondensation of ε-caprolactam under normal atmosphere, in which obvious agglomeration of SNWs can be found. The SNW loading in the control composite is 5.0 wt %.

Interface interaction between SNW and PA6 matrix

Interfacial affinity has been found to be one of the most important factors in determining the mechanical properties of composites. Good interaction at interface can improve the mechanical properties of composites, but poor interactions may lead to an increase of defects at interface and, further, premature material fracture under low load.[35]

Because of the presence of amide groups in PA6 chains, chemical bonding such as hydrogen bonding can be easily formed at the interface between PA6 matrix and polar inorganic fillers, such as silicate or hydroxyapatite. Of course, for stoichiometric silicon nitride with N/Si molar ratio of 1.333, it cannot form hydrogen bonding with PA6 at interface because it does not contain oxygen or hydrogen. However, the atoms in outermost layer of SNW are highly reactive because the N and Si are in unsaturated state. Therefore, SNW can quickly react with oxygen or water upon exposure to air even at room temperature,[36,37] as shown in Figure 6. So, the surface layer of commercial silicon nitride has a significant amount of functional groups, such as Si_2—NH, Si—NH_2, and Si—OH.[38,39] The reaction mechanism has been discussed in great detail by Brow and Pantano,[37] and the presence of these groups on the surface of silicon nitride particles has been confirmed by X-ray photoelectron spectroscopy.

Because of the presence of these polar groups on the surface of SNW, there may be two kinds of interaction models relevant for the PA6/SNW system. First, the polar groups present on the SNW surface can form hydrogen bonds with the amide groups of PA6, according to the scheme shown in Figure 7. Second, some PA6 chains may be grafted to the surface of SNWs via covalent bond. This model is

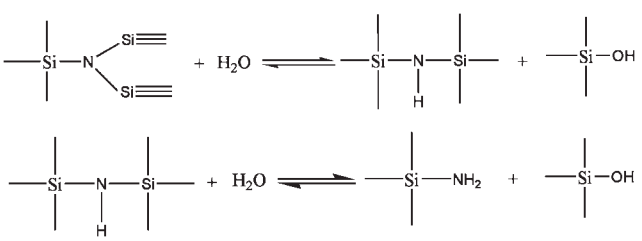

Figure 6 The formation mechanism of polar groups on the surface of SNWs.

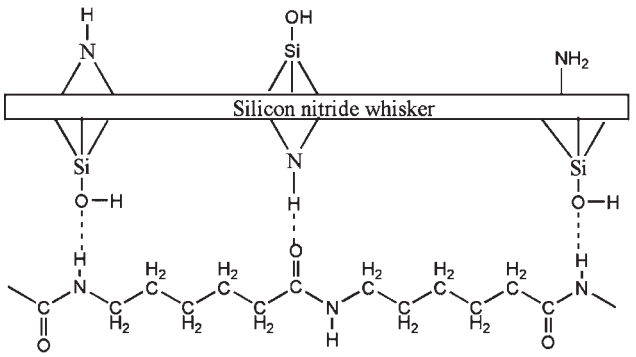

Figure 7 Schematic diagram of hydrogen bonding between SNWs and PA6. The dashed line represents hydrogen bonds.

mainly based on the presence of amine groups on the surface of SNWs and the reactivity of these $-NH_2$ groups with carboxyl groups. It is clear that the PA6 synthesized via polymerization of ε-caprolactam always has an end carboxyl group. When the $-NH_2$ groups present on the surface of SNWs react with the end carboxyl groups of PA6, some PA6 chains can be grafted on the surface of SNWs via covalent bond, as shown in Figure 8.

To confirm the fact that some PA6 chains have been grafted on SNWs, SNWs were separated form PA6/SNW composite by a procedure mentioned previously and characterized using FTIR. Figure 9 shows the FTIR spectra of SNWs separated from PA6/SNW composites and as-received SNWs. In Figure 9(A), the pronounced absorption band with maximum at 974 cm^{-1} is assigned to the backbone vibration of Si—N—Si. In addition to the characteristic peak of silicon nitride, some other peaks also appear in the FTIR spectrum of SNW, which means that other groups are also present on the SNWs. The band at about 3422 cm^{-1} arises from νOH +νNH combination band.[38] The absorption band at 1631 cm^{-1} is assigned to the N—H shear vibration. The

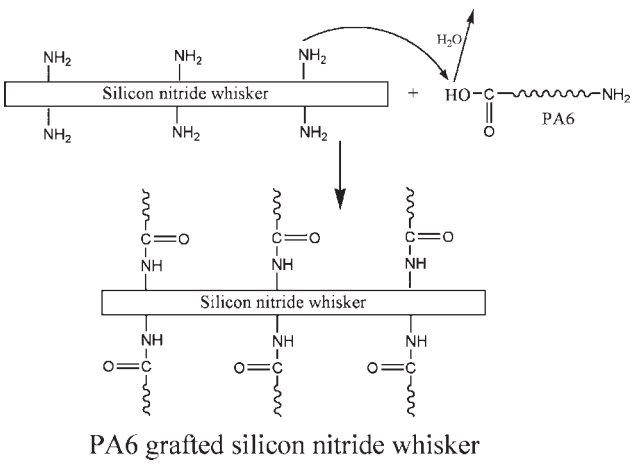

Figure 8 Overall scheme for the grafting of PA6 on SNWs.

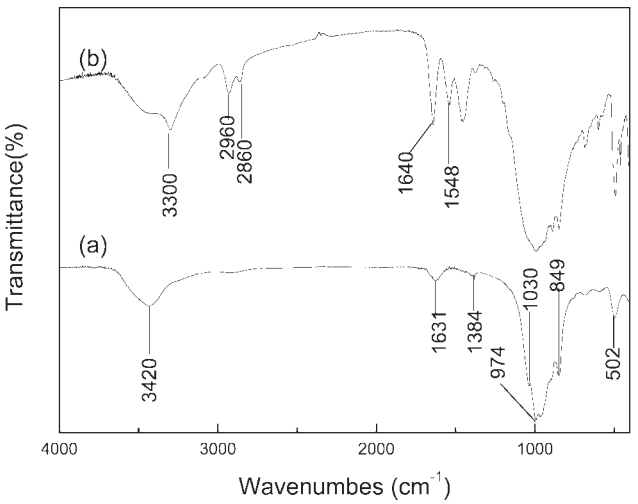

Figure 9 FTIR spectra of (a) SNWs and (b) SNW-*g*-PA6.

band at 1384 cm^{-1} is attributed to the bending mode of hydroxyl groups.[40] The absorption at 1030 cm^{-1}, as well as a broad and weak band at 502 cm^{-1} in Figure 9(A), is probably indicative of the presence of SiO_2. From the analysis, it is clear that the SNWs used in this study really contain a large amount of polar groups.

In Figure 9(B), in addition to the absorption peaks corresponding to SNW, the most prominent peaks occur at about 3300, 2960, 2860, 1640, and 1548 cm^{-1}. The band at 3300 cm^{-1} arises from the hydrogen-bonded N—H stretch of PA6. The two bands at 2960 and 2860 cm^{-1} confirm the existence of $-CH_2-$. The band at 1640 cm^{-1} is assigned to the amide I C=O mode of PA6. The existence of these characteristic peaks of PA6 confirms that the surface of SNWs is coated with a layer of PA6.[35] Considering that the sample was washed many times before testing and free PA6 has been washed away completely, it can be concluded that the PA6 molecules are connected with the surface of silicon nitride whiskers by covalent bond instead of physical absorption.

Figure 10 shows the SEM images of the impact fracture surface of PA6SNW-5, from which the morphology of SNWs pulled out from PA6 matrix can be clearly observed. It can be seen that PA6 matrix is strongly attached to the SNW at the bottom. In addition, the surface of SNW is covered with a layer of PA6 matrix, which makes the surface of SNWs looks very coarse. This morphology reflects that strong adhesion exists at the interface between SNWs and PA6 matrix.

Mechanical properties

The $\overline{M}_w$ and $\overline{M}_w/\overline{M}_n$ of PA6, PA6/SNWs, and the control composite have no obvious difference (as

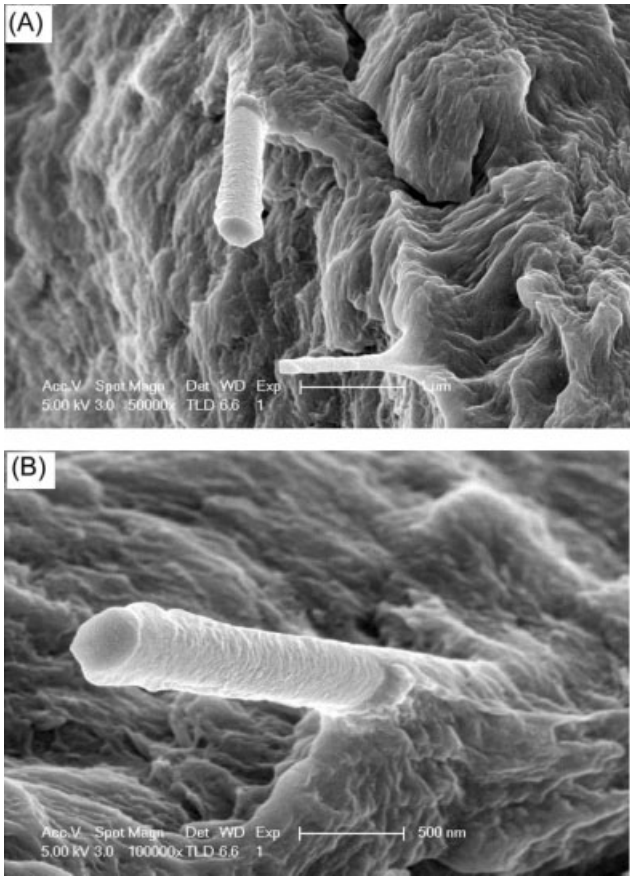

Figure 10 SEM images of SNWs from PA6 matrix, showing the strong interface interaction.

shown in Table II). Therefore, it is feasible to compare their mechanical properties.

The results of tensile and flexural tests are summarized in Table III, and the representative stress–strain curves of PA6, control composite, and PA6/SNW composites are shown in Figure 11.

Compared with pure PA6, it can be seen from Table III and Figure 11 that the tensile strength, flexural strength, and modulus of PA6/SNW composites are considerably increased by the incorporation of SNWs, although elongation at break decreases. The decreased elongation at break may originate from the formation of microvoids because of debonding of whiskers from the polymer matrix upon failure, as is often the case with nanofiller-reinforced polymer composites.[41] The flexural strength, flexural modulus, tensile strength, and tensile modulus of PA6SNW5 are 132, 3200, 91.3, and 2889 MPa, respectively, which are 60.3, 73.9, 37.9, and 80.5% higher than those of pure PA6. The obvious mechanical property improvement confirms the excellent reinforcing effect of SNWs on PA6.

TABLE II
Weight-Average Molecular Weight ($\overline{M}_w$) and Distribution ($\overline{M}_w/\overline{M}_n$) of PA6, PA6SNWs, and the Control Composite

Sample code	$\overline{M}_n$ (kg/mol)	$\overline{M}_w$ (kg/mol)	$\overline{M}_w/\overline{M}_n$
PA6	13.6	21.4	1.57
PA6SNW1	14.0	21.8	1.56
PA6SNW3	14.5	23.1	1.59
PA6SNW5	14.8	22.8	1.54
Control composite	14.7	22.8	1.55

The excellent reinforcing effect of SNW on PA6 can be attributed to the strong interface interaction and the superhigh strength and modulus of SNW. Attention should also be paid to the comparison of mechanical properties between PA6SNW5 and the control composite. Although the SNW loading in these two composites is identical, the strength and modulus of the control composite are much lower than that of PA6SNW5. For example, the tensile strength of the control composite is 76.6 MPa, which is 14.3 MPa lower than that of PA6SNW5. There are four factors that mainly influence the reinforcing effect of filler: the strength and toughness of fillers, the shape of fillers, the interface between fillers and matrix, and the dispersion state of filler in matrix. The former three factors are identical to both PA6SNW5 and the control composite. Therefore, the big difference in mechanical properties can be mainly attributed to the different dispersion state of whiskers in these two samples. As confirmed by SEM previously, the SNWs are uniformly dispersed in PA6SNW5. Therefore, almost each whisker can function as stress-bearing backbone. However, in the control composite, SNWs mainly exist in the form of

TABLE III
Tensile and Flexural Properties of PA6, Control Composite, and PA6/SNW Composites

	Tensile			Flexural	
Material	Strength (MPa)	Modulus (MPa)	Elongation at break (%)	Strength (MPa)	Modulus (MPa)
PA6	66.2	1600	120	82.3	1840
PA6/SNW1	73.4	2143	34.2	101	2350
PA6/SNW3	82.2	2543	27.5	118	2860
PA6/SNW5	91.3	2889	23.3	132	3200
Control composite	76.6	2457	9.4	121	2950

large agglomerates. Therefore, these whiskers cannot bear stress synchronously and evenly.

Because of the elongated shape and super high strength, whiskers are effective in bridging microcracks and preventing them from propagating into macrocracks.[12] Therefore, the incorporation of single-crystal whiskers into polymer often contributes to an increased toughness of the composite, which has been widely confirmed by many researchers, and the toughening mechanism of whiskers on polymers has also been elucidated in some literatures.[42]

The results of Izod notched impact test are shown in Figure 12. It can be seen that the impact strength of PA6SNW composites increases obviously with the increasing loading of SNW, indicating that SNW has good toughening efficiency on PA6. In particular, the notched impact strength of PA6SNW5 is 128 J/m, which is 64% higher than that of pure PA6 (78 J/m) and also 34.7% higher than that of the control composite (95.4 J/m). The higher impact strength of PA6SNW5 compared with the control composite can be attributed to the uniform dispersion of SNW.

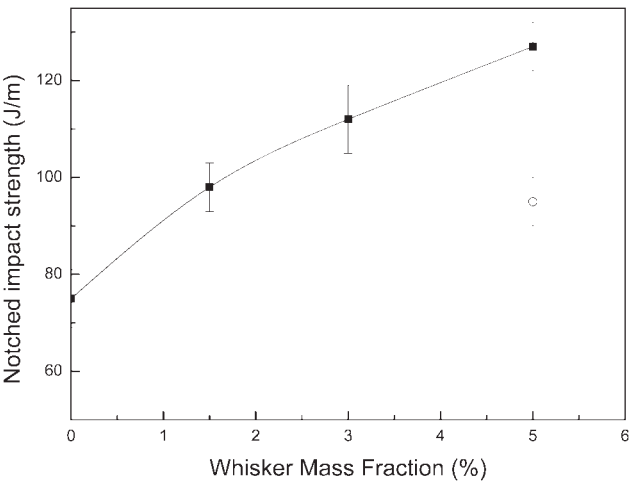

Figure 12 Notched impact strength of the PA6SNW composites as a function of SNW loading. Values of the control composites are shown with open symbols. Each value is the mean with error bar showing one standard deviation (SD) of six measurements ($n = 6$).

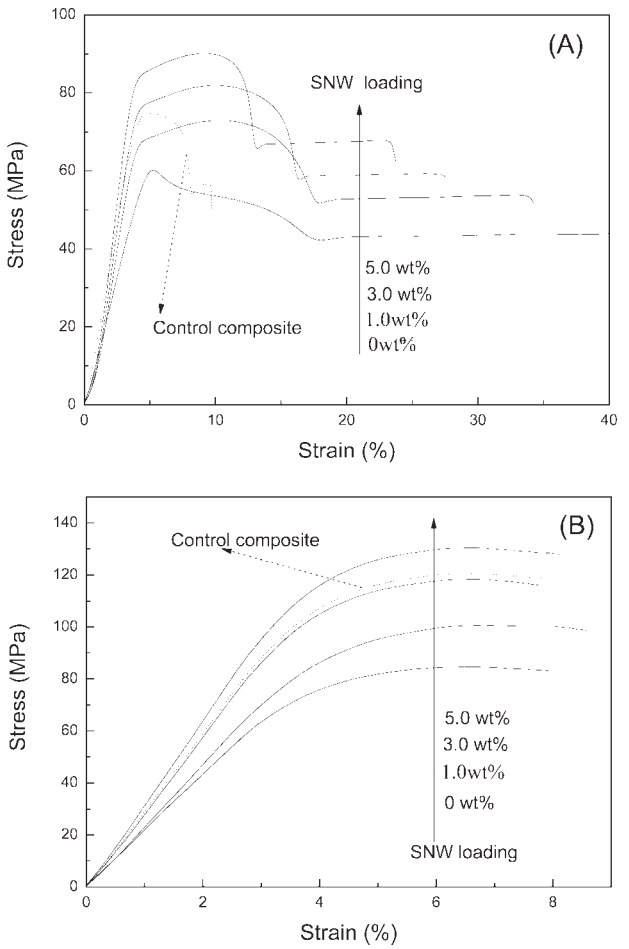

Figure 11 Representative stress–strain curves of PA6, PA6SNW composites with different SNW, and the control composite. (A) Tensile stress–stain curves and (B) flexural stress–strain curves.

CONCLUSIONS

PA6/SNW composites were prepared via *in situ* hydrolytic ring-opening polymerization of ε-caprolactam. The reinforcing and toughening efficiency of SNW on PA6 was evaluated.

IS-HROP is an effective method to fabricate PA6/whisker composite with uniform dispersion. The success of this method mainly lies in the fact that the polymerization is performed in the presence of high-temperature boiling water, which can effectively prevent SNWs from precipitating and agglomerating and also help disentangle the agglomerates of whiskers.

FTIR analysis reveals that a large amount of polar groups, such as —NH, —SiOH, and —NH_2 groups, are present on SNW. Hydrogen bonds can be formed at interface between these polar groups and the amide groups of PA6. Besides, some PA6 chains have been grafted on the SNW surface via the condensation reaction between the amine groups present on SNW and the end carboxyl groups of PA6.

The incorporation of SNW can remarkably increase not only the strength and modulus but also the impact strength of PA6, which can be mainly attributed to the superhigh strength, modulus, good toughness of silicon nitride, and strong interface interaction between PA6 matrix and SNW. However, the excellent reinforcing efficiency of SNWs can be displayed only when they are dispersed uniformly in PA6 matrix. Otherwise, the reinforcing effect of SNWs would be decreased because of the severe agglomeration and entanglement of whiskers.

References

1. Xu, H. H.;Martin, T. A.; Antonucci, J. M.; Eichmiller, F. C. J Dent Res 1999, 78, 706.
2. Tjong, S. C.; Jiang, W. J Appl Polym Sci 1999, 73, 2985.
3. Liang, G. Z.; Hu, X. L. Polym Int 2004, 53, 670.
4. Tjong, C.; Jiang, W. J Appl Polym Sci 1999, 73, 2247.
5. Urayama, H.; Ma, C. H.; Kimura, Y. Macromol Mater Eng 2003, 288, 562.
6. Liang, G. Z.; Hu, X. L. J Appl Polym Sci 2004, 92, 1950.
7. Persson, A. L.; Schreiber, H. P. J Polym Sci Part B: Polym Phys 1997, 35, 2457.
8. Shi, J.; Wang, Y.; Gao, Y.; Bai, H. W. Compos Sci Technol 2008, 68, 1338.
9. Wang, B. B.; Zhou, Z. W.; Gu, L. X. Mater Res Bull 2003, 38, 1449.
10. Zhou, Z. W.; Liu, S. K.; Gu, L. X. J Appl Polym Sci 2001, 80, 1520.
11. Xu, H. H.; Eichmiller, F. C.; Antonucci, J. M.; Schumacer, G. E.; Ives, L. K. Dent Mater 2000, 16, 356.
12. Xu, H. H.; Quinn, J. B.; Smith, D. T.; Giuseppetti, A. A.; Eichmiller, F. C. Dent Mater 2003, 19, 359.
13. Xu, H. H.; Smith, D. T.; Schunmacher, G. E.; Eichmiller, F. C. J Biomed Mater Res 2000, 52, 812.
14. Wang, Q. H.; Xue, Q. H.; Shen, W. C. J Appl Polym Sci 1998, 69, 2341.
15. Chen, J.; Chen, P.; Wu, L. C.; Zhang, J.; He, J. S. Polymer 2006, 47, 5402.
16. Xue, Q. J.; Zhang, Z. Z.; Liu, W. M.; Shen, W. C. J Appl Polym Sci 1998, 69, 1393.
17. Tjong, S. C.; Meng, Y. Z. J Appl Polym Sci 1999, 72, 501.
18. Zhuang, G. S.; Sui, G. X.; Meng, H.; Sun, Z. S.; Yang, R. Compos Sci Technol 2007, 67, 1172.
19. Tjong, S. C.; Meng, Y. Z. Polymer 1999, 40, 7275.
20. Tjong, S. C.; Meng, Y. Z. J Appl Polym Sci 1998, 70, 431.
21. Meng, Y. Z.; Tjong, S. C. Polymer 1999, 40, 1109.
22. Lv, J. Z.; Lu, X. H. J Appl Polym Sci 2001, 82, 368.
23. Phillip, B. M.; Obrez, A.; Lindberg, A. J Prosthet Dent 1998, 79, 278.
24. Wen, Z. Y.; Wu, M. M.; Itoh, T.; Kubo, M.; Lin, Z. X.; Yamamoto, O. Solid State Ionics 2002, 148, 185.
25. Xu, Y. S.; Chung, D. D.; Mroz, C. Compos A 2001, 32, 1749.
26. Sato, N.; Kurauchi, T.; Sato, S.; Kamigaito, O. J Mater Sci 1991, 26, 3891.
27. Nair, S. V.; Shiao, M. L.; Garrett, P. D. J Mater Sci 1992, 27, 1085.
28. Malzahn, J. C.; Friederich, K. J Mater Sci 1984, 3, 861.
29. Pecorini, T. J.; Hertzberg, R. W. Polym Eng Sci 1994, 15, 174.
30. Joseph, K.; Pavithran, C.; Brahmakumar, M. J Appl Polym Sci 1993, 47, 1731.
31. Garcia, R. M.; Cavaille, J. Y.; Dupeyre, D.; Peguy, A. J Polym Sci Part B: Polym Phys 1994, 32, 1437.
32. Iwanaga, H.; Kawai, C. J Am Ceram Soc 1998, 81, 773.
33. Huttinger, K. J.; Pierchnick, T. W. J Mater Sci 1994, 29, 2879.
34. Ou, Y. C.; Yang, F.; Chen, J. J Appl Polym Sci 1997, 64, 2317.
35. Li, L. J.; Yang, G. S. Polym Int 2008, 57, 1226.
36. Castanho, S. M.; Moreno, R.; Fierro, J. L. J Mater Sci 1997, 32, 157.
37. Brow, R. K.; Pantano, C. G. J Am Ceram Soc 1987, 70, 9.
38. Baraton, M. I.; Chang, W.; Kear, B. H. J Phys Chem 1996, 100, 16647.
39. Batan, A.; Franquet, A.; Vereecken, F. Surf Interface Anal 2007, 40, 754.
40. Yao, C.; Gao, G.; Lin, X. O.; Yang, X. J.; Lu, L.; Wang, X. Mater Chem Phys 1986, 14, 123.
41. Pavlidoua, S.; Papaspyrides, C. D. Prog Polym Sci 2008, 33, 1119.
42. Taesler, C. H. R.; Wittich, H.; Jurgens, C.; Schulte, K.; Krichel-dorf, H. R. J Appl Polym Sci 1996, 61, 783.